Two-dimensional Laminar-Flow Analysis, Utilizing a Doubly Refracting Liquid

JOHN W. PRADOS and F. N. PEEBLES

University of Tennessee, Knoxville, Tennessee

An experimental technique for the determination of velocity distributions in two-dimensional laminar flow is described. The method utilizes the optical interference patterns observed in flowing doubly refracting liquids when viewed by transmitted polarized light. The fluid shear-stress distribution may be determined from these interference patterns by methods similar to those employed in solid photoelasticity. Methods are presented for the calculation of velocity distributions from the observed stress distributions. Experiments are described in which the technique was applied to determine velocity profiles in parallel-walled, converging and diverging channels and for flow about a cylindrical obstacle. The doubly-refracting liquids employed were aqueous solutions of an organic dye. Independent experimental checks were obtained in most instances, and these are in satisfactory agreement with the calculated results.

For many years the photoelastic technique has been a powerful tool for experimental stress analysis in solids. This technique is based on the fact that certain substances become temporarily doubly refracting (that is, anisotropic to the passage of light) when subjected to shearing stresses. When a doubly refracting substance is viewed by transmitted light between two polarizing plates, visible interference patterns are produced, which are related to the material dimensions and properties and to the shearing stresses in the specimen. The method has been used extensively in the analysis of two-dimensional stress systems, and special techniques permit the analysis of certain three-dimensional systems. A complete and readable treatment of photoelastic theory and practice is given by Frocht (*8*).

An analogous phenomenon in liquids was reported by J. C. Maxwell in 1873 (*16*) and has been the subject of extensive investigation since. General reviews of this work have been presented by Cerf and Scheraga (*5*), Peebles, Prados, and Honeycutt (*19*), Edsall (*7*), and others. In liquids the phenomenon has been called *streaming birefringence, streaming double refraction,* or *flow double refraction.* The last name is preferred by the present authors.

By far the largest portion of the investigations on flow double refraction has concerned its application to the study of molecular size and shape. However, as early as 1923, Humphry (*13*) showed the possibility of using doubly refracting liquids as tools for the visual analysis of flow.

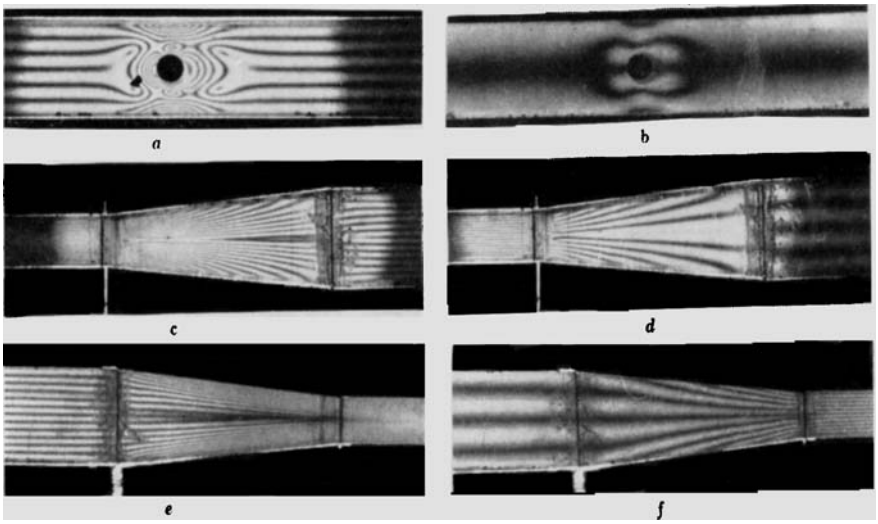

Fig. 1. Typical light interference patterns produced by flow double refraction in aqeuous milling yellow solutions.

- ***a.*** **Flow about a cylindrical obstacle at an intermediate flow rate, circularly polarized light.**
- ***b.*** **Flow about a cylindrical obstacle at a low flow rate, plane polarized light.**
- ***c.*** **Flow in a diverging channel at a high flow rate, circularly polarized light.**
- ***d.*** **Flow in a diverging channel at a low flow rate, circularly polarized light.**
- ***e.*** **Flow in a converging channel at a high flow rate, plane polarized light.**
- ***f.*** **Flow in a converging channel at a low flow rate, plane polarized light.**

Visible interference patterns are observed when a doubly refracting liquid is caused to flow through a transparent channel between polarizing plates and viewed by transmitted light. These patterns are composed of alternate light and dark bands which appear stationary in steady laminar flow but take on a random eddying motion in turbulent flow. The bands are of two types: isochromatics which are related to the magnitude of the maximum shearing stress in the liquid, and isoclinics, which are related to the direction of the maximum shearing stress. Peebles and Prados (*20*) have shown the conditions necessary to produce light interference (and hence a dark band) for both the isochromatic and isoclinic cases. The two types of bands may be distinguished by the observation of a given flow situation in both plane and circularly polarized light. The isochromatics alone appear in circularly polarized light, while both isochromatics and isoclinics appear in plane polarized light.

F. N. Peebles is with Union Carbide Nuclear Company, Oak Ridge, Tennessee.

The intensity of the doubly refracting behavior is expressed in terms of the amount of double refraction, a measure of the relative velocities of light rays vibrating in different directions in the anisotropic medium. It can be shown that an isochromatic band appears whenever the amount of double refraction and fluid depth along the light path are such that the light transmitted through the liquid undergoes a relative retardation equal to an integral number of wave lengths. The amount of double refraction is a single-valued, increasing function of shear stress for a given doubly refracting liquid. Hence for a given depth of a given liquid there is a fixed value of shear stress associated with each isochromatic band in the interference pattern. This makes possible a quantitative determination of the shear-stress distribution from the interference patterns in a doubly refracting liquid, provided the liquid has first been calibrated by the determination of the relationship between shear stress and amount of double refraction. The method of calibration described by Peebles and Prados (*20*) consists of subjecting the liquid to known shear stresses, viewing it in polarized light, and observing the formation of the isochromatic bands. A similar procedure yields the relationship between isoclinic bands and stress directions. This relationship is expressed in terms of the extinction angle, which relates the stress direction necessary for light extinction to the axis of polarization of the incident light.

Flow double refraction provides an excellent qualitative way to study laminar, turbulent, or transition (unstable) flows. Regions of local turbulence, vortices, boundary layers, and the like are clearly defined. Stroboscopic illumination is useful in observing turbulent flow behavior. However attempts to use the technique for quantitative determination of velocity profiles have proved successful only for the case of two-dimensional laminar flow. Photographs of typical two-dimensional laminar-flow situations are shown in Figure 1.

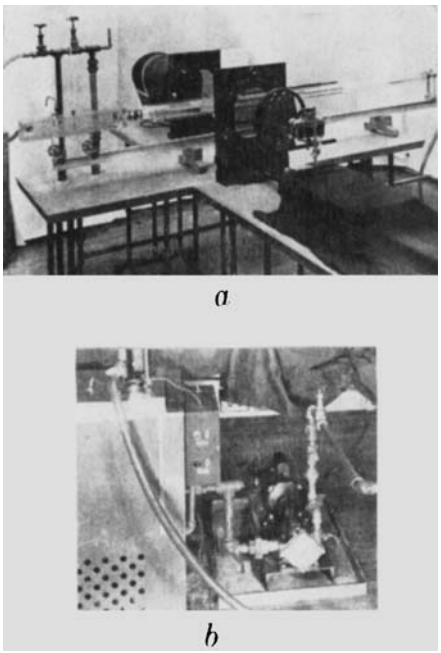

Fig. 2. Photographs of the flow facility: *a.* flow test channel, calming box and optical components, *b.* pump and constant-temperature bath.

PREVIOUS INVESTIGATIONS

Prior applications of the technique of flow double refraction to the analysis of fluid motion have been relatively few in comparison with the large volume of literature dealing with flow double refraction in general. It is felt that some mention of these studies and the doubly refracting liquids employed is in order at the present time.

The earliest such application appears to have been due to Humphry (*13*) in 1923. Using a colloidal sol of vanadium pentoxide in water, he was able to demonstrate qualitatively the difference between laminar and turbulent flow. Further qualitative studies along these lines were the work of Leaf (*14*) in 1945, who employed doubly refracting bentonite sols in a locomotive fire box design, and the recent visual studies of Binnie (*3, 4*) and Lindgren (*15*) on the transition from laminar to turbulent flow in tubes. The last two investigators used aqueous sols of benzopurpurin and bentonite respectively.

Attempts to obtain quantitative measurements of velocity profiles with flow double refraction were first made by Alcock and Sadron (*1*) in 1936. Their doubly refracting liquid was sesame oil, which is highly viscous and has a low optical sensitivity but is more stable over periods of time than the colloids previously employed.

By far the most extensive of the quantitative investigations were those reported by Hauser and Dewey (*6, 10, 11*) between 1940 and 1942. Using bentonite sols they made quantitative and qualitative studies of velocity profiles in two-dimensional laminar flow. However in the analysis of their results two questionable assumptions were made: that the isoclinics were related to streamline direction rather than shear-stress direction and that the isochromatics were a function of the velocity gradient normal to the streamlines rather than the shearing stress in the liquid. Some calculations presented by Rosenberg (*22*) and experimental observations made during the present investigation do not support these assumptions.

Weller *et al.* (*28, 29*) in 1943 carried out some studies similar to those of Hauser and Dewey using a solution of ethyl cellulose in a commercial solvent, Methyl Cellosolve, instead of bentonite. Ullyott (*26*) in 1947 described work similar to that of Hauser and Dewey and of Weller but made no attempt to interpret his results quantitatively.

A careful study of fluid-flow analysis by the double-refraction technique was presented in 1952 by Rosenberg (*22*), who showed that the direction of maximum shear stress in fluids and the direction of the streamlines are not coincident except for the case of parallel streamlines and suggested a method for the analysis of a general two-dimensional flow situation in which the streamlines are not parallel. No experimental measurements were reported by Rosenberg, nor did he carry out any actual flow analyses, but some of his suggestions have been extended and incorporated into the present work.

Recent investigations of interest are those of Wayland (*27*) and of Thurston and Hargrove (*24*). Wayland studied the flow in the annular space between fixed and rotating cylinders and reported quantitative results for the laminar-flow region; he employed bentonite sols and pure ethyl cinnamate as doubly refracting liquids. Wayland was also able to demonstrate a correlation between the amount of double refraction in pure ethyl cinnamate and the shear stress for turbulent flow. It should be noted that his doubly-refracting liquid had an optical sensitivity considerably lower than that of the liquids employed in the present investigation, and so isochromatics as such did not appear. Instead a compensator was used to measure the amount of double refraction. Such a technique would be essential for studies of turbulent flow, since under such conditions the fringes break up into swirling regions of light and dark and no longer have a fixed location. The studies of Thurston and Hargrove are concerned with the pulsating flow of fluids through circular orifices. Their work utilizes

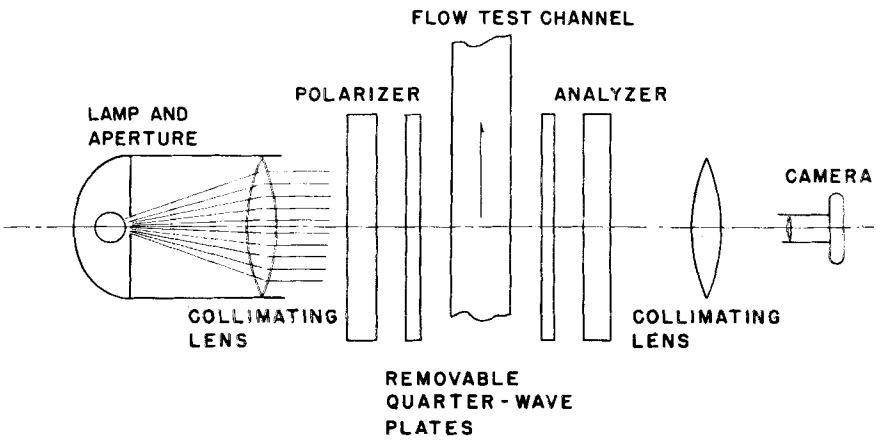

Fig. 3. Schematic representation of the optical system.

an aqueous solution of milling yellow dye as the working fluid and is apparently the first recorded attempt to apply the technique of flow double refraction to unsteady or pulsating flow.

METHOD OF APPROACH

It was felt that the flow double refraction method offered unique advantages for the analysis of complex two-dimensional laminar-flow situations, and the present work was undertaken in an attempt to overcome some of the previous difficulties and place the analysis of results on a sounder basis. Specifically the objectives were twofold: the development of mathematical techniques for flow analysis from double refraction measurements based on more general assumptions than those previously employed, and the application of these techniques to the experimental analysis of a number of two-dimensional laminar-flow situations. It was also desired to check the experimental results by independent means wherever possible.

To achieve these objectives a mathematical analysis was made to relate desired flow parameters to quantities which could be obtained from flow double refraction measurements. Next an experimental study was carried out for three types of two-dimensional laminar flow: flow between parallel plates, where the streamlines are straight and parallel; flow in convergent and divergent channels, where the streamlines are straight but not parallel; and flow about a cylindrical obstacle, where the streamlines are neither straight nor parallel. The results were interpreted in the light of the mathematical analysis, and use was also made of some suggestions by Rosenberg (*22*) which enable one to avoid the questionable assumptions of former investigators.

The doubly refracting liquid used in the present study was an aqueous solution of a commercially available organic dye, milling yellow. Stable, satisfactory working solutions of this dye can be prepared with viscosities not over twenty times that of water. They exhibit marked flow double refraction in concentrations as low as 1.2% dye by weight. Their use in flow studies was first reported by Peebles, Garber, and Jury (*18*).

MATHEMATICAL RESULTS

It should be emphasized here that the present study is based on the assumption that the amount of double refraction at a point in a doubly refracting liquid in two-dimensional laminar flow is a single-valued function of the maximum shear stress at that point. This has been well justified experimentally in the case of photoelastic solids, but previous investigations involving doubly refracting liquids have not been of such a nature as to confirm or deny the concept. It was further assumed that the extinction angle was a single-valued function of the maximum shear stress at any point in a two-dimensional laminar-flow field.

To carry out a flow analysis under these assumptions it is necessary to have two relationships: that between the maximum shear stress and the velocity gradient normal to the streamlines of flow and that between the direction of action of the maximum shear stress and the direction of the streamlines. These expressions are developed in the Appendix* and are

$$\frac{\partial V}{\partial n} = \frac{V}{r} \pm \sqrt{E^2 - \frac{4V^2}{r'^2}} \qquad (1)$$

$$\theta = \phi - \tfrac{1}{2} \arctan\left(\frac{D}{G}\right) \qquad (2)$$

Equation (2) shows that the streamline directions coincide with the direction of maximum rate of deformation only for cases where the rate of dilation is zero; that is, the normal curves to the streamlines are straight lines, an indication that the streamlines are parallel and that no convergence or divergence of flow is occurring. If one takes only principal values for the arctangent, it is seen that the maximum difference in these directions which can occur is $\pi/4$ radians and will be manifested in situations where the rate of pure shear $[(\partial V/\partial n) - (V/r)]$ is zero but the rate of dilation $(-(2V/r'))$ is not. Such a situation would be found along the center line of a symmetrical convergent or divergent channel.

Equation (2) indicates that if the isoclinic positions are determined by the maximum rate of deformation, as results of the present study suggest, they will be of little use in determining the streamline patterns in cases where convergence or divergence of the flows occurs. Hence Equation (1) can be used to determine the velocity distribution only for cases where the streamline pattern is known from the channel configuration, where it is known that no divergence or convergence of flow occurs and the streamline patterns can be developed from the isoclinics, or where the streamline patterns can be obtained from some source other than double refraction measurements. The use of Equation (1) in some specific situations will be illustrated.

CALCULATION OF VELOCITY DISTRIBUTIONS FOR SPECIFIED CASES

Case I: Parallel Straight Streamlines

For laminar flow between flat plates the streamlines are straight and parallel. This situation is approximated experimentally by flow in a straight rectangular channel of high aspect ratio (ratio of

*Tabular material has been deposited as document 5872 with the American Documentation Institute, Photoduplication Service, Library of Congress, Washington 25, D. C., and may be obtained for $2.50 for photoprints or $1.75 for 35-mm. microfilm.

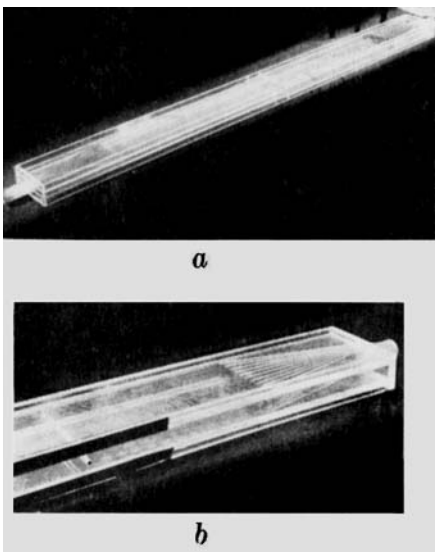

Fig. 4. Photographs of the flow test channel: *a.* flow test channel before installation of the cylindrical obstacle, *b.* deep end of channel showing flow diffuser vanes and cylindrical obstacle installed.

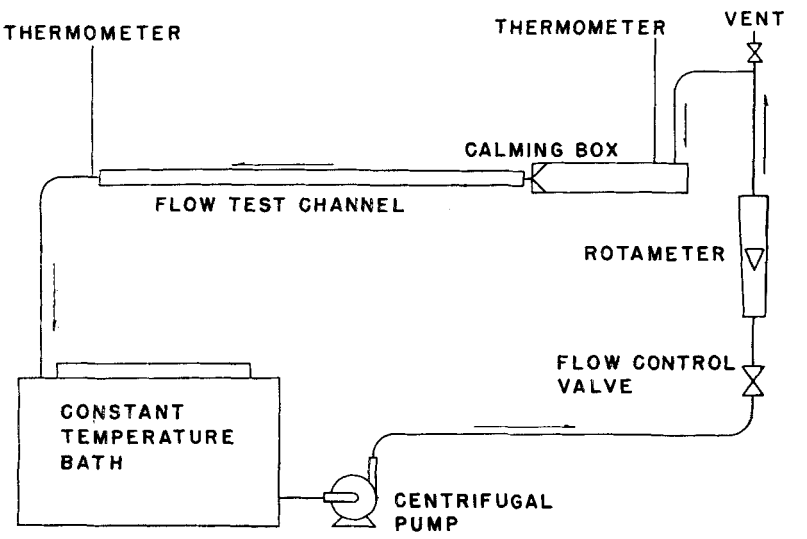

Fig. 5. Schematic representation of the fluid circulating system.

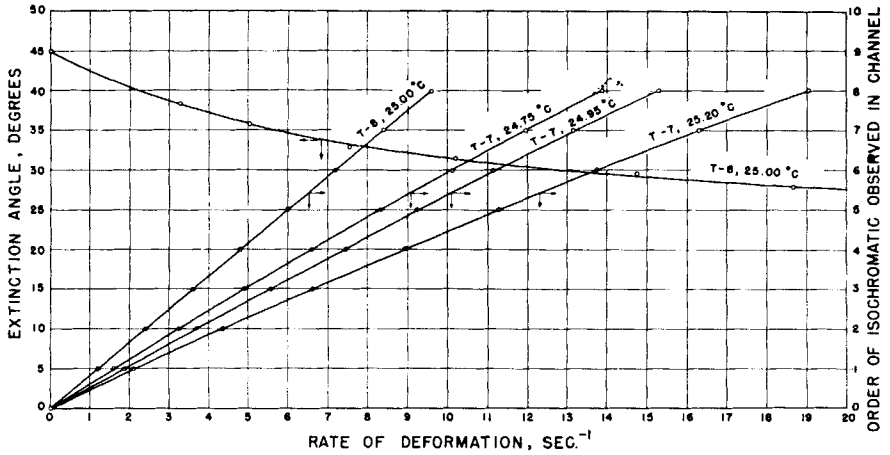

Fig. 6. Optical calibration curves for test solutions T-7 and T-8.

width to depth). In this case the terms V/r and V/r' vanish and the streamlines are determined by the channel walls. Equation (1) reduces to

$$\frac{dV}{dn} = \pm E \qquad (3)$$

From isochromatic patterns E may be specified throughout the field of flow. Equation (3) can then be integrated numerically or graphically along a stream normal to obtain the velocity distribution. Necessary boundary conditions are provided by the fact that $V = 0$ at the channel walls.

Case II: Parallel Curved Streamlines

For the case of parallel but curved streamlines $V/r' = 0$ and $\theta = \phi$. Hence the isoclinic patterns may be used to obtain the streamlines throughout the flow field. A graphical or numerical method will be needed to determine their radius of curvature at each point. Equation (1) becomes

$$\frac{\partial V}{\partial n} = \pm E + \frac{V}{r} \qquad (4)$$

Having calculated r from the isoclinics and determined E from the isochromatics for each point in the field, one may integrate Equation (4) numerically to obtain the velocity distribution. Integration is performed along a streamline normal, subject to the boundary conditions of zero velocity at the walls.

Case III: Nonparallel Straight Streamlines

Flow between the two nonparallel walls provides a situation in which the streamlines are straight but not parallel, and the dilation component of the flow does not vanish. A good approximation to this case in practice is found in a symmetrical convergent (divergent) section joining two rectangular channels of the same width but different depths. One considers that the streamlines are radial lines emanating from the line at which the nonparallel walls would converge, if extended.

In the present case Equation (1) reduces to

$$\frac{\partial V}{\partial n} = \pm\sqrt{E^2 - \frac{4V^2}{r'^2}} \qquad (5)$$

which must be integrated numerically along a normal curve (here the arc of a circle whose center is the point of convergence of the walls). E is obtained from the isochromatics and r' from the channel configuration. The usual boundary conditions of zero velocity at the walls are used, and a check is provided in the fact that $\partial V/\partial n$ should vanish at the center of the channel for a symmetrical situation.

Case IV: General Two-Dimensional Flow with Known Streamlines

Situations may arise in which the streamlines are neither straight nor parallel but are known throughout the flow field from some source other than double-refraction measurements. One can obtain r and r' by a graphical or numerical method throughout the field and then apply Equation (1) directly. Numerical integration is performed along a streamline normal, subject to the zero-velocity conditions at the walls.

Case V: General Two-Dimensional Laminar Flow with Unknown Streamlines

Where the streamline distribution is unknown, Equation (1) is not suitable for calculation of velocity distributions. However a method of analyzing such cases has been proposed by Rosenberg (*22*). The analysis requires introduction of the Stokes stream function, which when inserted into the laminar-flow relationships yields the following equation:

$$\frac{\partial^2\Psi}{\partial x^2} - \frac{\partial^2\Psi}{\partial y^2} = E\cos 2\theta \qquad (6)$$

An important property of the stream function should be noted at this point; the difference in Ψ values between two points in the field of flow is numerically equal to the volumetric flow rate across any curve connecting the points. Two direct consequences of this property are that curves of constant stream-function values are the streamlines themselves and that the stream function is constant along any solid boundary. Furthermore for the case of unidirectional flow the value of Ψ may be obtained across a flow channel by direct integration.

Hence if one considers a situation in which the flow starts out as unidirec-

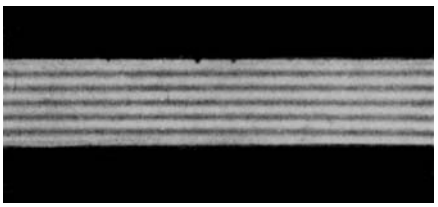

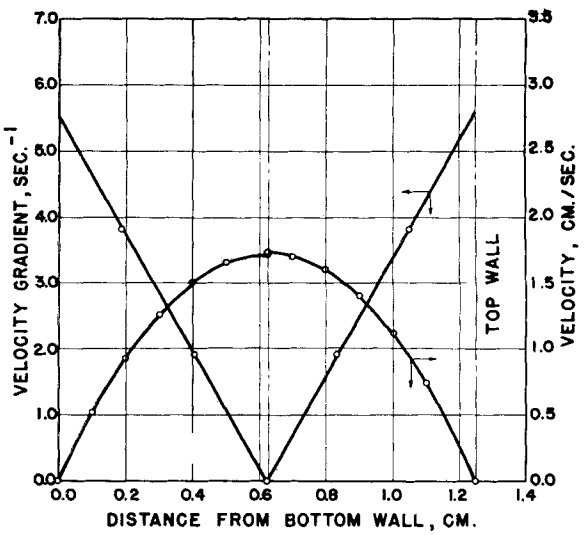

Fig. 7. Flow pattern photograph and plots of velocity gradient and velocity vs. distance for a straight channel of 10:1 aspect ratio: channel depth 1.250 cm., solution calibration T-7, 25.00°C.; measured discharge 18.1 cc./sec.; calculated discharge 18.1 cc./sec.

tional in a straight channel, he may assign an arbitrary value to Ψ along one of the channel boundaries and calculate the distribution of Ψ across to the other by integration. Having the value of Ψ along both channel boundaries and across the channel at some distance upstream from the region of interest, one has the necessary boundary conditions to begin a numerical solution of the second-order partial-differential equation (6). The values of E and θ may be obtained throughout the field of flow from the isochromatic and isoclinic patterns, respectively.

Numerical solution of Equation (6) requires that it first be placed in finite difference form. If one assumes that the flow field is divided up into a square grid of equal spacing in both x and y directions, the following difference equation results:

$$\Psi(x + h, y) + \Psi(x - h, y) - \Psi(x, y + h) - \Psi(x, y - h) = h^2 E \cos 2\theta \quad (7)$$

One may start from the known values of Ψ along the boundaries and employ a simple iteration procedure to obtain Ψ at each corner of the grid of spacing h. Graphical interpolation may be applied to determine curves of constant Ψ (streamlines), and numerical differentiation will yield the velocity components if desired.

APPARATUS

The experimental apparatus consisted of three major subsystems: the optical system, the flow test channel, and the fluid circulation system. Figure 2 shows over-all views of the equipment.

The optical system consisted of an Exakta 35-mm. single-lens reflex camera and standard polariscope components. The polariscope components were a light-source assembly consisting of interchangeable sodium vapor and tungsten lamps and a collimating lens, two polarizing plates mounted on ball-bearing rollers so that their axes of polarization might be varied at will, two quarter-wave plates mounted on sliding tracks to permit ready insertion in or removal from the light path, and a two-section optical bench. A 10-in. field of view was provided by this system. All optical components were mounted on two rigid tables, between which was placed a third table containing the flow test channel. The camera mount was a heavy platform fitted with a vertical rod and an adjustable clamp which held an adapter screwed into the tripod fitting of the camera; the arrangement of these components can be seen in Figures 2a and 3.

Photographs of the flow-test channel are shown in Figure 4. The channel was made of ⅜-in.-thick Plexiglas and provided a rectangular cross section for flow. The aspect ratio (ratio of width to depth) was kept high in order to approximate more closely a two-dimensional flow situation. Flow patterns were observed through the wide dimension of the channel as indicated in Figure 2.

The channel consisted of two sections of uniform rectangular cross section, one measuring 12.41 by 2.545 cm., the other 12.49 by 1.250 cm. These were joined by a straight-walled converging section. The converging section was symmetrical about the center line of the two uniform sections, and the converging walls made an angle of 5 deg. and 58 min. with the horizontal. Diffuser vanes were provided at each end of the system to spread the flow across the wide dimension and aid in rapid establishment of the two-dimensional velocity profiles. The channel was mounted on an aluminum rail and attached to an upstream calming box and downstream return line with short sections of rubber radiator hose. The hose was secured with circular clamps, and the entire assembly could be moved back and forth along the rail.

This test channel provided an opportunity for observing flow in uniform channels of different aspect ratios (5:1 and 10:1) and in straight convergent and divergent sections. In addition a 0.718-cm. O.D. cylindrical rod was inserted in the 2.545-cm.-deep section about midway along its length. The rod was mounted perpendicular to the side walls of the channel and extended all the way across the flow path, thereby permitting a study of the two-dimensional flow about a cylindrical obstacle. These details may be observed in Figure 4.

The prime fluid-circulation system components were an Aminco 16-gal. constant-temperature bath and a ¾-hp. centrifugal pump. Flow lines were standard 1-in. brass pipe, and 1-in. O.D., ¾-in. I.D. Tygon hose. A rotameter was used for flow-rate measurements, and a precision thermometer

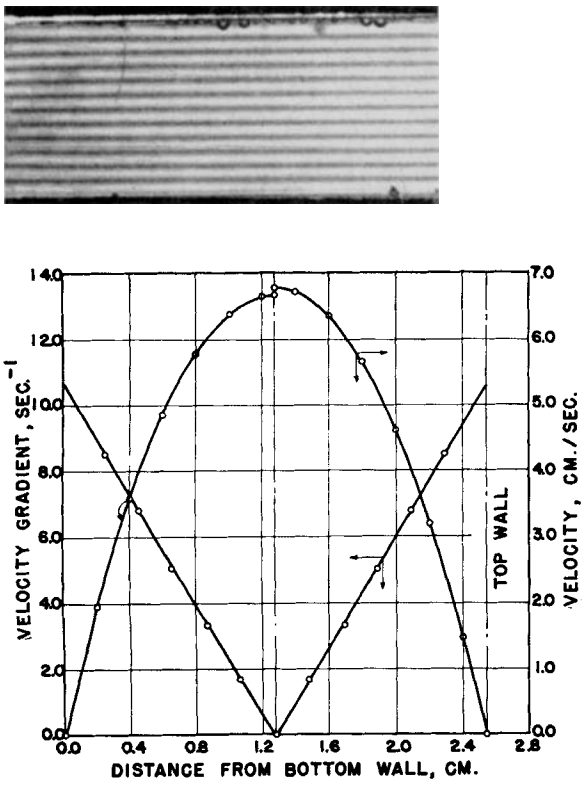

Fig. 8. Flow pattern photograph and plots of velocity gradient and velocity vs. distance for a straight channel of 5.1 aspect ratio: channel depth 2.546 cm.; solution calibration T-7, 24.80°C.; measured discharge 143.3 cc./sec.; calculated discharge 142.1 cc./sec.

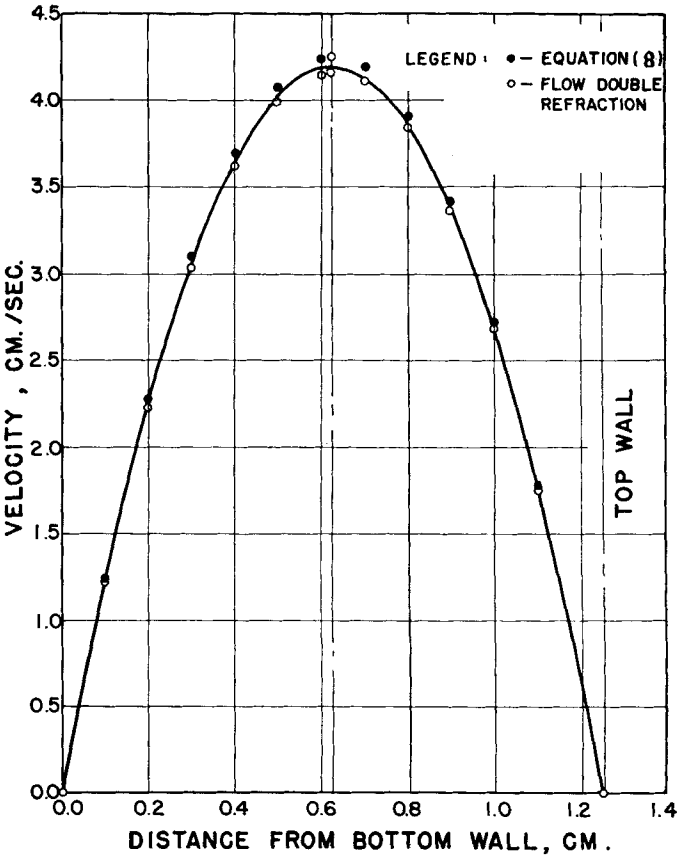

Fig. 9. Comparison of velocity profiles calculated from Equation (8) and obtained from flow double refraction measurements.

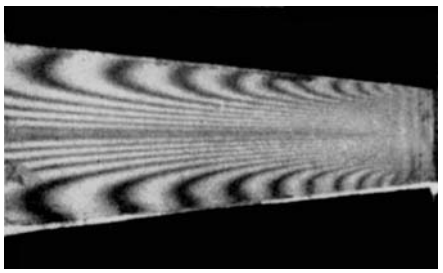

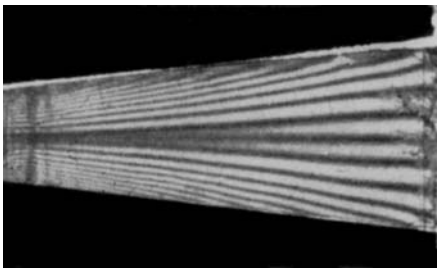

of considerable importance to the final photographic results, since each negative was enlarged to approximately 200 times its original area. Photographs were obtained for flow in shallow and deep straight-channel sections, in the converging and diverging sections, and about the cylindrical obstacle.

Most of the photographs of the iso-

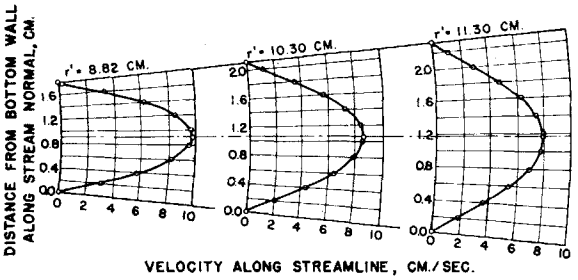

Fig. 10. Photograph and developed profiles for flow in a diverging channel: solution calibration T-7, 24.85°C.; measured discharge 134.6 cc./sec.; calculated discharge $r' = 8.81$ cm., $r' = 10.31$ cm., $r' = 11.31$ cm., $Q = 136.4$ cc./sec., $Q = 138.7$ cc./sec., $Q = 139.7$ cc./sec.

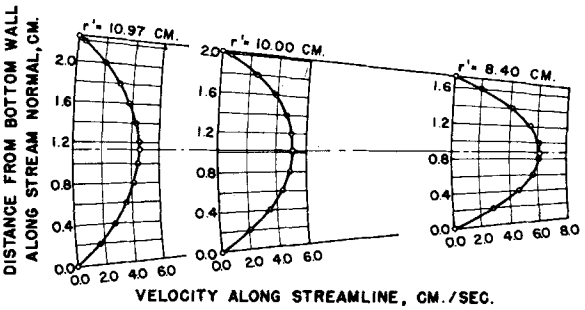

Fig. 11. Photograph and developed velocity profiles for flow in a converging channel: solution calibration T-7, 24.90 C.; measured discharge 81.2 cc./sec.; calculated discharge $r' = 8.40$ cm., $r' = 10.00$ cm., $r' = 10.97$ cm., $Q = 91.5$ cc./sec., $Q = 91.9$ cc./sec., $Q = 8.88$ cc./sec.

reading to 0.05°C. was mounted in the calming box just upstream from the flow channel. The arrangement is shown schematically in Figure 5.

The dye solutions themselves were prepared from commercial lots of milling yellow NGS powder. The manner of preparation and optical calibration is described by Peebles and Prados. Viscous properties of the solutions were determined in a variable-head capillary viscometer similar in principle to that described by Maron, Krieger, and Sisko (*17*). A complete description of the viscometry technique used in the present investigation is given by Havewala (*12*).

EXPERIMENTAL WORK

Photographs were made of the interference patterns over a wide range of flow rates for the available geometries, that is, straight channel flow, converging and diverging flow, and flow about the cylindrical obstacle. The optical components were carefully aligned before each run, and the fluid temperature was maintained at 25.00 ± 0.15°C. in the calming box just upstream from the test section. Flow rate and temperature were recorded for each photograph taken.

The optimum exposure time and lens aperture were obtained by trial and error for each film used. The following appeared to give the best results for the isochromatic photographs.

Film	Exposure time, sec.	Lens stop
Tri-X	1.0	Between 11 and 16
Plus X	4.0	Between 11 and 16
Micro File	12.0	8

The Microdol developer used produced a photograph of fine grain, which was chromatic patterns were made with circularly polarized, monochromatic light, that is, with quarter-wave plates in place and the sodium vapor lamp in use. Some isochromatic patterns, particularly in the convergent and divergent sections, were photographed with monochromatic plane-polarized light by sliding the quarter-wave plates out of the light path. In all cases the axis of polarization of the polarizer was vertical and that of the analyzer was horizontal.

In photographing the isoclinic patterns it was necessary to use white light, so that the black isoclinics might be distinguished from the colored isochromatics. Plane-polarized light of various orientations was provided by rotating the polarizer and analyzer together, keeping them crossed all the while. Isoclinic photographs were made for flow about a cylindrical obstacle at various orientations of polarizer and analyzer, but at a single flow rate and fluid temperature. The polarizer and analyzer were rotated together in a counterclockwise direction (looking toward the light source). Photographs were made at rotations of 0, 15, 30, 45, 60, 75, 90, and −15 deg. The −15- and 75-deg. patterns were identical, as were the 0- and 90-deg. patterns.

Because of marked changes over a period of 2 weeks in the optical response of the solutions while they remained in the flow system, samples were withdrawn on each day that photographs were made. These were stored in glass bottles for later calibration. Previous tests had shown that milling yellow solutions stored in glass bottles underwent no measurable

VERTICAL COORDINATE	0	1	2	3	4	5	6	7	8	9	10	11	12	13	14	15	16	17	18
8	-3.59 -1.900	-3.59 -1.900	-3.61 -1.900	-3.72 -1.900	-4.05 -1.900	-4.62 -1.900	-6.09 -1.900	-8.19 -1.900	-9.50 -1.900	-9.50 -1.900	-8.33 -1.900	-6.27 -1.900	-4.99 -1.900	-4.32 -1.900	-3.82 -1.900	-3.67 -1.900	-3.60 -1.900	-3.59 -1.900	-3.59 -1.900
7	-2.62 -1.731	-2.62 -1.731	-2.58 -1.733	-2.52 -1.726	-2.50 -1.712	-2.51 -1.700	-1.81 -1.648	-2.55 -1.326	-4.39 -1.261	-4.70 -1.367	-4.35 -1.520	-3.80 -1.489	-3.05 -1.632	-2.62 -1.685	-2.62 -1.712	-2.62 -1.730	-2.62 -1.730	-2.62 -1.733	-2.62 -1.731
6	-1.72 -1.299	-1.72 -1.299	-1.62 -1.296	-1.51 -1.290	-1.19 -1.273	-0.080 -1.206	1.32 -0.943	2.60 -0.751	0.68 -0.348	0.16 -0.441	0.50 -0.769	0.76 -0.867	0.42 -0.965	-0.26 -1.179	-1.00 -1.250	-1.38 -1.277	-1.55 -1.298	-1.70 -1.296	-1.72 -1.299
5	-0.82 -0.690	-0.82 -0.690	-0.83 -0.692	-0.64 -0.690	0.74 -0.663	0.99 -0.508	2.04 -0.443	2.56 -0.228	3.00 -0.049	3.58 -0.072	3.70 -0.150	2.57 -0.322	1.37 -0.457	0.76 -0.504	0.67 -0.643	-0.51 -0.678	-0.71 -0.686	-0.79 -0.692	-0.82 -0.690
4	0 0	0 0	0 0	0 0	0 0	0 0	0 0	0 0			0 0	0 0	0 0	0 0	0 0	0 0	0 0	0 0	0 0
3	0.82 0.690	0.82 0.690	0.81 0.687	0.64 0.688	-0.83 0.659	-0.97 0.449	-2.84 0.450	-4.49 0.153	-3.00 -0.048	-3.36 0.159	-1.47 0.286	-1.03 0.419	-0.93 0.476	-0.66 0.517	-0.65 0.629	0.35 0.673	0.73 0.685	0.78 0.687	0.82 0.690
2	1.70 1.294	1.70 1.294	1.62 1.296	1.48 1.281	1.20 1.268	0.21 1.207	-0.67 0.947	-1.35 0.853	-0.63 0.548	-0.70 0.585	-0.56 0.727	-1.71 0.866	-0.64 1.030	0.72 1.172	1.02 1.259	1.41 1.259	1.62 1.289	1.70 1.296	1.70 1.294
1	2.62 1.726	2.62 1.726	2.62 1.724	2.54 1.726	2.60 1.707	2.81 1.698	3.21 1.678	4.29 1.467	5.05 1.502	3.84 1.483	3.92 1.454	3.18 1.511	2.63 1.627	2.77 1.699	2.73 1.719	2.70 1.729	2.68 1.726	2.62 1.724	2.62 1.726
0	3.61 1.893	3.61 1.893	3.69 1.893	3.72 1.893	4.20 1.893	4.77 1.893	6.12 1.893	8.22 1.893	9.50 1.893	9.60 1.895	8.48 1.893	6.63 1.893	5.31 1.893	4.53 1.893	4.03 1.893	3.83 1.893	3.68 1.893	3.61 1.893	3.61 1.893

HORIZONTAL COORDINATE

Fig. 12. Tabulation of values of the x component of the rate of deformation and the stream function at the corners of the coordinate grid.

change in optical or viscous properties during periods of at least 3 months. In the present study all calibrations were performed within 3 weeks after the photographs were made. Optical calibration curves for the test solutions used are presented in Figure 6.

The positions of isochromatic and isoclinic bands were obtained from accurate measurements made from enlargements

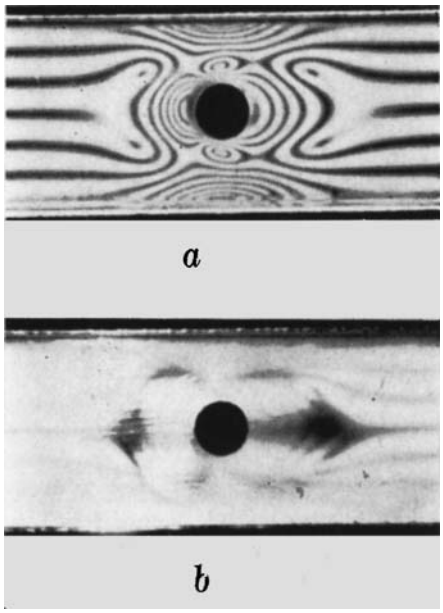

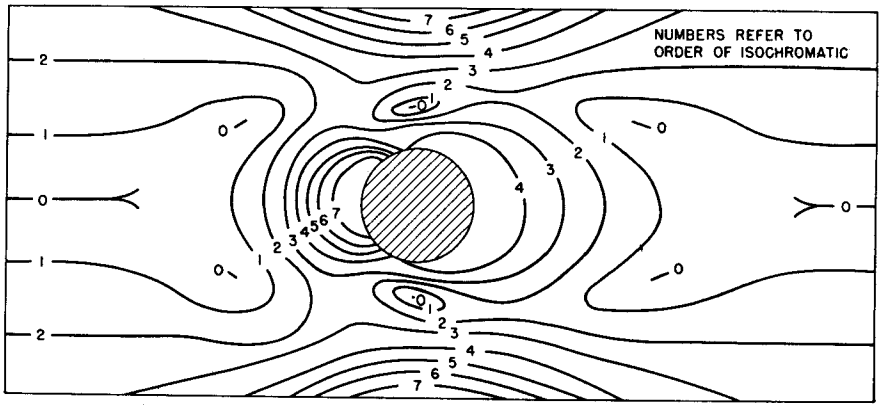

(c)

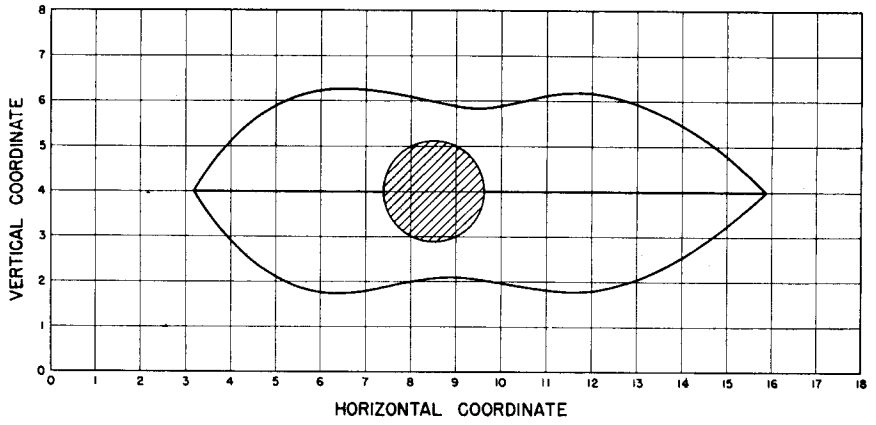

(d)

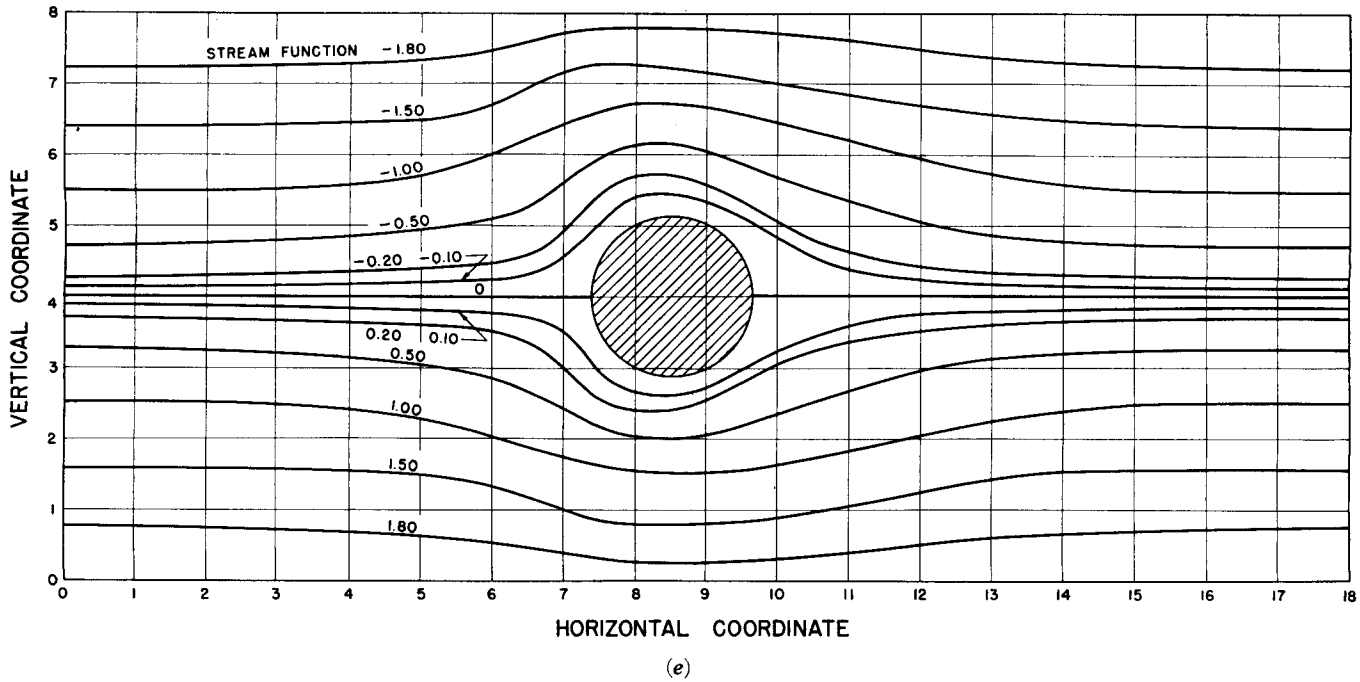

(e)

Fig. 13. Steps in the development of streamlines about a cylinder: *a.* isochromatic photograph; *b.* isoclinic photograph, 0, 90; *c.* isochromatic tracing; *d.* isoclinic traced from *b*; *e.* developed streamlines about cylinder.

of the flow-pattern photographs. Distance-scale ratios were determined with the known distance from top to bottom of the channel used as a reference. A detailed description of the methods used in the measurements is given by Prados (*21*).

FLOW ANALYSIS FROM PHOTOGRAPHIC MEASUREMENTS

The procedures used to analyze the photographic measurements follow. As these differed for the three types of flow studied, each will be discussed separately.

Straight Parallel Flow

The measurements taken from the photographs of straight parallel flow gave the location of each isochromatic along a vertical line from the top to the bottom of the flow channel. From the optical calibration curve for the test liquid a

rate of deformation was associated with each isochromatic, and hence the rate of deformation could be plotted vs. distance across the channel. Such photographs and plots are shown in Figures 7 and 8.

For straight parallel flow the rates of deformation and velocity gradient are equal. Hence graphical integration of the curve of rate of deformation vs. distance was used to obtain a similar curve of values of velocity vs. distance across the channel. This unidirectional velocity-distribution curve was then integrated to yield the total discharge through the channel. The results of these calculations for the cases illustrated in Figures 7 and 8 are tabulated in Tables 1 and 2.*

In addition the velocity distribution in the 10:1 aspect-ratio channel was compared with that calculated from viscous information. The results of the viscosity determinations showed that the test solutions used behaved as Newtonian fluids with viscosities of 17.1 and 26.5 centipoises at rates of deformation from 2 to 12 reciprocal sec. (the range of interest of the present investigation). Peebles *et al.* (*19*) have found that at shear stresses above 20 dynes/sq. cm. milling yellow solutions exhibit marked pseudoplasticity. They have also shown however that at low shear stresses the viscous behavior should become Newtonian, which is in accordance with experimental observation. Hence the formula for velocity distribution of a Newtonian fluid flowing between two parallel plates

$$u = \frac{3Q}{4ab}\left[1 - \left(\frac{y}{a}\right)^2\right] \qquad (8)$$

was assumed to hold for the high-aspect-ratio channel and was used to calculate the velocity profile.

Agreement between velocities calculated from Equation (8) and the flow double refraction measurements was excellent. A comparison of the two is shown in Figure 9.

Converging and Diverging Flow

Photographic measurements of convergent and divergent flow gave the isochromatic positions along circular arcs centered at the hypothetical point of convergence of the nonparallel channel walls. The rate of deformation along such an arc could be obtained from the optical calibration curve of the test liquid, but here the velocity gradient was no longer equal to the rate of deformation. The velocity profile could be obtained however by direct numerical integration of Equation (5) subject to the boundary conditions of zero velocity at the walls. Integration was carried out by the method of Runge and Kutta as given by Scarborough (*23*). The results of such integrations at three locations along a divergent channel are shown graphically in Figure 10 and are tabulated in Table 3*.

*See footnote p. 227.

Similar results for flow in a convergent channel are given in Figure 11 and Table 4.*

Since flow across a closed curve in two dimensions is equal to the velocity component normal to the curve multiplied by the length of curve, the discharge through a converging or diverging channel of high aspect ratio can be calculated from the expression

$$Q = b\int_0^N V\,dn \qquad (9)$$

Discharges calculated from Equation (9) are given in Figures 10 and 11.

Flow About a Cylindrical Obstacle

From the measured positions of the isochromatic and isoclinic bands one may determine the maximum rate of deformation and angle made by this maximum rate with the horizontal from the flow photographs. These values were found at each corner of a square grid of 144 points, 18 units along the channel by 8 units across the channel. The value of the component of deformation acting in the positive x direction was found from the following relationship, which follows directly from Equation (34) (see Appendix).*

$$E_{xy} = E\cos 2\theta \qquad (10)$$

The needed quantities were obtained from the extinction angle, isoclinic angle, and isochromatic fringes. The values of E_{xy} obtained at the corners of the grid are tabulated in Figure 12. The values were then used in the numerical integration of Equation (6), which was integrated in difference form [Equation (7)] and required as boundary conditions the values of Ψ along the top and bottom of the channel and along two adjacent vertical grid lines upstream and two downstream from the obstacle. These values were obtained as follows.

*See footnote in column 1.

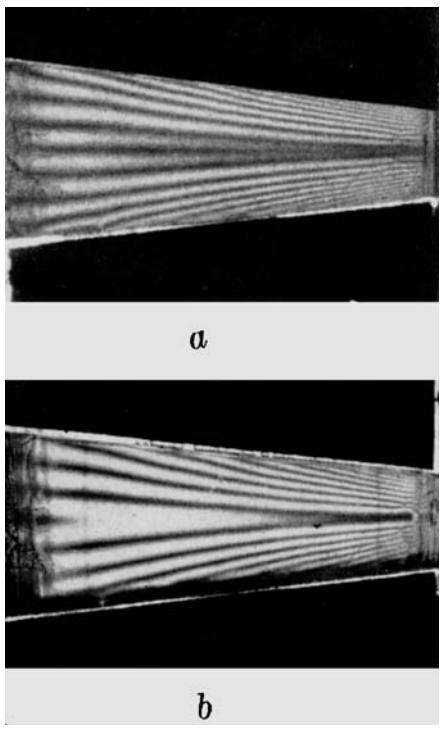

Fig. 14. Flow patterns produced in a converging channel from plane and circularly polarized light at comparable flow rates: *a.* plane polarized light, circularly polarized light.

For undisturbed unidirectional flow the stream function can be calculated across the channel from

$$u = \frac{-d\Psi}{dy}\,; \qquad \Psi(y) = \Psi(0) - \int_0^y u\,dy \qquad (11)$$

Since Ψ may be specified with reference to an arbitrary constant only, the value of Ψ was chosen as zero at the center of the channel, and other values of Ψ out to the top and bottom walls were calculated from Equation (11). Then use was made of the fact that Ψ is constant along streamlines and solid boundaries. This immediately specified Ψ along the top and bottom of the channel and from symmetry considerations along the center line of the channel and the cylinder boundary as well.

The nature of Equation (7) necessitated iteration which started along both upstream and downstream edges of the grid and worked toward the middle. The results of the iteration process are shown in tabular form in Figure 12. Graphic interpolation was used to determine curves along which Ψ has a constant value. These are the streamlines of flow about the obstacle. The photographs and curves of Figure 13 illustrate the steps in the development of these streamlines from the flow photographs. Calculation procedures and intermediate results are given by Prados (*21*).

Unfortunately the results of the calculation could not be checked by calculating the discharge, since the flow through the channel was already fixed by fixing the values of the stream function along the boundaries. A number of theoretical results for flow of a viscous fluid about a cylinder were examined, but they were all developed either for the case of unbounded flow (*2*) or for a Reynolds number of the order of 0.1 (*25*). The Reynolds number obtained for the present situation was 3.81, calculated by

$$N_{Re} = \frac{dU\rho}{\mu} \qquad (12)$$

The viscous drag coefficient for flow about the cylinder was calculated as illustrated in the Appendix. Again checking was hampered by the lack of avail-

able measurements in the literature for flow about a cylinder in a closely bounded channel. The value of the viscous drag coefficient of 1.83 obtained from double-refraction measurements was compared with the experimental value of 2.0 given by Goldstein (*9*) for flow in an unbounded channel at the same Reynolds number. The value of 1.86 calculated from the expression of Bairstow *et al.* (*2*) for flow in a bounded channel at Reynolds numbers less than 0.1 gave better agreement.

SUMMARY OF RESULTS AND DISCUSSION

Tables 5 and 6* summarize the agreement obtained between measured and calculated flow rates for the straight channels, converging channel, and diverging channel. Original data, from which these and all other results reported in this paper are compiled, are given by Prados (*21*). For the straight channels the agreement between measured and calculated flow rates was within +7.3, −9.6%, with a mean square deviation of 4.22%. For the convergent and divergent flows agreement was within +13.2, −11.2%, with a mean square deviation of 7.75%. Twenty-six straight-channel runs and fourteen converging and diverging runs were analyzed. Only one calculation was made for the flow about the cylinder.

An examination of the interference patterns in a convergent or divergent channel by means of both plane- and circularly polarized light as shown in Figure 14 yields some extremely interesting results in support of the present analysis. As can be seen from Figure 14*b*, the pattern given by circularly polarized light has no zero-order isochromatic along the center of the channel. If the amount of double refraction were dependent only upon the rate of pure shear, as has been suggested by some investigators (*6, 7, 19, 29*), including the authors, there would certainly be a zero-order isochromatic along the center of the channel, for here the rate of pure shear vanishes. On the other hand the rate of dilation does not vanish, and hence the total rate of deformation is not zero. Therefore the nonappearance of the zero-order isochromatic tends to support the conclusion that the amount of double refraction is a function of the total rate of deformation (or the maximum shear stress) for the doubly refracting liquids employed in the present study.

Figure 14*a* made in plane-polarized light does show a dark band along the center line of the channel. This might lead one to suppose that it is, indeed, a zero-order isochromatic. However since the isochromatic must appear in circularly polarized light as well as in plane-polarized light, one must conclude that this band is an isoclinic. When one recalls Equation (2) and notes that G vanishes at the center of the convergent channel while D does not, it is seen that here

$$\theta = \phi \pm \frac{\pi}{4} \qquad (13)$$

with the sign determined by whether the rate of shear approaches zero from above or below the center line of the channel. Equation (13) states that the plane of maximum shear stress makes an angle of 45 deg. with the horizontal streamlines at the center of the convergent and divergent channels. The total maximum rate of deformation is quite low, however, and the extinction angle is approximately 45 deg. Hence an isoclinic appears along the channel center line. If the optical orientation of the doubly refracting liquid were determined by the streamlines, other circumstances would occur. The horizontal streamline makes an angle of 90 deg. with the vertical plane of polarization of the incident light; the extinction angle is 45 deg., and hence no isoclinic would appear. Since the isoclinic does appear, it may be concluded that the optical orientation of the doubly refracting milling yellow solutions is determined by the direction of the maximum shear stress (or rate of deformation) rather than the streamline direction.

Since the method of treating the data from the double-refraction measurements involved two integrations, it would be expected that any random errors in the measurements of the fringe locations themselves would tend to be averaged out and their effect minimized. There were several possible sources of error however which would not be so affected: misalignment of optical components due to the optical bench being made in two sections rather than one, difference between the temperature indicated by the thermometer upstream from the test section and the actual temperature in the test section itself, personal errors in reading the rotameter or thermometer, and nonparallelism of the channel walls. The effect of errors from these sources is very difficult to estimate. An additional source of error was introduced into the converging and diverging flow calculations by the graphical determination of the radius of curvature of the stream normal.

Because of the lack of an adequate method of checking results it is difficult to assess the validity of the streamline patterns developed about the cylindrical obstacle. The pattern as shown in Figure 13 satisfies one's intuitive notion as to how such a flow should look. The wider separation of the streamlines on the downstream side suggests the existence of a stable pair of vortices directly behind the cylinder. To demonstrate these from flow double-refraction measurements, it would be necessary to refine the coordinate grid considerably, near the cylinder. Unfortunately the isochromatic patterns are quite faint and distorted in this region, and it is doubtful that any consistent results could be obtained even if the grid were refined.

To obtain any precise indication of flow next to an obstacle of this nature it will probably be necessary to modify the details of channel construction somewhat. As pointed out by Frocht (*8*) for the case of photoelastic solids, the production of sharp, accurate double-refraction patterns next to solid boundaries requires that all corners be square and surfaces parallel within very close tolerances. In spite of extreme care exercised in the construction of the Plexiglas channels it is doubtful that the required tolerances could be attained, and there was no convenient way to check this internally after the channel had been assembled. Another difficulty arose in the fixing of the cylindrical obstacle in the channel itself. To prevent leaks a rather tight fit was required, and some small amounts of residual stress were set up in the Plexiglas about the cylinder mount. Since Plexiglas is doubly refracting when stressed, this resulted in further distortion of the interference pattern in the immediate vicinity of the cylinder.

Another possible source of error, therefore, was double refraction in the Plexiglas channel walls. However, it is not believed that this would seriously affect the present results, since with the fluid at rest the flow channel appeared uniformly dark, indicating that no appreciable double refraction was occurring along the light path. A faint lightening of the field was observable within $\frac{1}{16}$ in. of the cylindrical obstacle, but its effect was confined to a region in which no fringes could be clearly observed.

In addition to these sources of error the isoclinic patterns were somewhat diffuse, and it was difficult to locate accurately the center line of a given isoclinic curve for tracing (see Figure 13). This may again have been due in part to nonparallelism of the channel walls or to a slight misalignment of the optical components.

In view of these difficulties it is rather encouraging to note the fairly close agreement in stream-function values at the meeting point for calculations started upstream and downstream from the cylinder (see Figure 12). The agreement, within 2%, of the drag coefficients calculated from flow double refraction and the theoretical formula of Bairstow (*2*) is also encouraging, although there is considerable uncertainty as to the effect produced by the use of Bairstow's formula at a Reynolds number of 3.81, which is considerably higher than the maximum value of 0.1 for which it was derived.

It is hoped that eventually a more accurate check on these results can be made by the determination of the streamline patterns for flow about a cylindrical obstacle by some method other than

*See footnote p. 227.

from flow double-refraction measurements. Direct injection of a dark-dye or a stream of tiny air bubbles would enable one to trace out the streamline pattern and compare it with that obtained in the present work as shown in Figure 13.

CONCLUSIONS AND RECOMMENDATIONS

From the results of the investigation, the following conclusions have been drawn.

1. The experimental quantities furnished by the flow double-refraction technique may be analyzed to yield the streamline and velocity distribution in a two-dimensional laminar-flow situation.
2. The results of such analyses are quantitatively accurate within $\pm 10\%$ for flow with straight, parallel streamlines and within $\pm 15\%$ for flow with straight, nonparallel streamlines.
3. Quantitative results may be obtained for a general two-dimensional flow situation involving neither straight nor parallel streamlines. Absolute determination of the limits of error on these results will require further experimental effort.

It is therefore felt that this technique will be of real use in the analysis of complex laminar-flow situations which can be idealized to two dimensions. The technique should be especially valuable in those situations where a measuring probe is undesirable, as in the narrow laminar boundary layers formed next to solid objects in a turbulent stream.

ACKNOWLEDGMENT

The authors wish to thank the Office of Naval Research for its support of the major portion of this investigation. Additional support from the Engineering Experiment Station and Department of Chemical Engineering of the University of Tennessee is also gratefully acknowledged.

NOTATION

a = distance from center to top or bottom of rectangular channel
b = width of rectangular channel
C_{Df} = viscous drag coefficient for circular cylinder
d = diameter of cylindrical obstacle
D = rate of dilation in a viscous fluid
D_f = viscous drag force, exerted in the direction of flow, on a unit length of circular cylinder with axis normal to the flow
E = maximum rate of deformation at a point in a viscous fluid
E_ξ = rate of deformation in a viscous fluid along a plane oriented at an angle ξ to the horizontal
E_{xy} = rate of deformation in a viscous fluid along a horizontal plane
f = focal length of camera lens
g_c = force-mass unit conversion constant
G = rate of pure shear in a viscous fluid
h = incremental distance in x and y coordinates for iterative solution of partial differential equation in difference form
n = stream normal coordinate, distance along a curve normal to a set of streamlines
N = total distance from wall to wall of channel taken along a stream normal
N_{Re} = Reynolds number
Q = volumetric discharge through flow channel
r = radius of curvature of a streamline
r' = radius of curvature normal to a set of streamlines
s = streamline coordinate, distance along streamline
t = time
u = fluid velocity component in x direction
U = mean flow velocity of fluid in a channel, that is, the ratio of volumetric discharge to channel cross-sectional area
v = fluid velocity component in y direction
V = fluid velocity along a streamline
x = horizontal coordinate-rectangular Cartesian system
y = vertical coordinate-rectangular Cartesian system

Greek Letters

β = polar angle inside circular cylinder
θ = angle made by direction of maximum shear stress with the horizontal in a moving viscous fluid
μ = fluid viscosity
ξ = angle measured from horizontal made by an arbitrary direction in a moving viscous fluid
π = ratio of circumference to the diameter of a circle
ρ = fluid density
σ_x = normal stress exerted in x direction in a moving viscous fluid
σ_y = normal stress exerted in y direction in a moving viscous fluid
τ = maximum shear stress at a point in a moving viscous fluid
τ_ξ = shear stress in a moving viscous fluid, acting on a plane oriented at angle ξ to the horizontal
τ_{xy} = shear stress acting in positive x direction on a surface facing in positive y direction in a moving viscous fluid
ϕ = angle made by a streamline with the horizontal
Ψ = Stokes stream function

LITERATURE CITED

1. Alcock, E. D., and C. L. Sadron, *Physics* **6**, 92 (1935).
2. Bairstow, L., B. M. Cave, and E. D. Lang, *Proc. Roy. Soc. (London)*, **A100**, 394 (1922).
3. Binnie, A. M., *Proc. Phys. Soc. (London)*, **57**, 390 (1945).
4. Binnie, A. M., and J. S. Fowler, *Proc. Roy. Soc. (London)*, **A192**, 32 (1947).
5. Cerf, Roger, and H. A. Scheraga, *Chem. Rev.* **51**, 185 (1952).
6. Dewey, D. R., Ph.D. dissertation, Mass. Inst. of Technol., Cambridge (1941).
7. Edsall, J. T., "Advances in Colloid Science," Vol. I, p. 269, Interscience, New York (1942).
8. Frocht, M. M., "Photoelasticity," Vol. I., John Wiley, New York (1941).
9. Goldstein, Sydney, "Modern Developments in Fluid Dynamics," Vol. I., The Clarendon Press, Oxford (1938).
10. Hauser, E. A., and D. R. Dewey, *Ind. Eng. Chem.*, **31**, 786 (1939).
11. ———, *J. Phys. Chem.*, **46**, 212 (1942).
12. Havewala, J. B., Bachelor's thesis, Univ. Tenn., Knoxville (1957).
13. Humphry, R. H., *Proc. Phys. Soc. (London)*, **35**, 217 (1923).
14. Leaf, Walter, *Mech. Eng.*, **67**, 586 (1945).
15. Lindgren, E. R., *Arkiv. Fysik.*, **7**, 293 (1954).
16. Maxwell, J. C., *Proc. Roy. Soc. (London)*, **22**, 46 (1873).
17. Maron, S. H., I. M. Krieger, and A. W. Sisko, *J. Appl. Phys.*, **25**, 971 (1954).
18. Peebles, F. N., H. J. Garber, and S. H. Jury, *Proc. Third Midwestern Conf. on Fluid Mechanics*, Univ. Minnesota Press, Minneapolis (1953).
19. Peebles, F. N., J. W. Prados, and E. H. Honeycutt, Jr., *Prog. Rep.* 1 and 3 under Contract Number Nonr-811(04), Eng. Expt. Sta. Univ. Tenn., Knoxville (1954).
20. Peebles, F. N., and J. W. Prados, paper in preparation.
21. Prados, J. W., Ph.D. thesis, Univ. Tenn., Knoxville (1957). Available on 35-mm. microfilm through University Microfilms, 313 N. First St., Ann Arbor Michigan, at a cost of $2.35.
22. Rosenberg, Benjamin, *Rept.* **617**, Navy Dept., David W. Taylor Model Basin, Washington 7, D. C., (1952).
23. Scarborough, J. B., "Numerical Mathematical Analysis," 3 ed., The Johns Hopkins Press, Baltimore (1955).
24. Thurston, G. B., and L. E. Hargrove, *Tech. Rept.* 1 and 4, Contr. DA-23-072-ORD-583, Office of Ordnance Research and the Research Foundation, Okla. Agr. Mech. Coll., Stillwater (1957).
25. Tomotiko, S. and T. Aoi, *Quart. J. Mech. and Appl. Math.*, **3**, 140 (1950).
26. Ullyott, Philip, *Trans. ASME*, **69**, 245 (1947).
27. Wayland, Harold, *J. Appl. Phys.*, **26**, 1197 (1955).
28. Weller, R., *J. Appl. Mech.*, **14**, 103 (1947).
29. Weller, R., D. J. Middlehurst, and R. Steiner, *Natl. Advisory Comm. Aeronaut. Tech. Note* 841 (1942).

Manuscript received January 23, 1958; revision received July 24, 1958; paper accepted October 1, 1958.